

Drift-Free Dynamic Height Sensor using MEMS IMU Aided by MEMS Pressure Sensor

Makoto Tanigawa, Henk Luinge, Linda Schipper, and Per Slycke (Xsens Technologies)

Abstract— We demonstrate a low-cost, low-power, and small form factor solution to drift-free high-resolution vertical positioning by fusing MEMS accelerometers with MEMS barometric altimeter. In this system, the highly responsive but drift-prone aspect of the MEMS accelerometers is stabilized by barometric altimeter and high-fidelity height tracking is achieved. Typical vertical human movements such as walking up or down a staircase can be tracked in real-time with this system. The height tracking performance is benchmarked against a reference system using a tactical-grade IMU and an error analysis is performed.

I. INTRODUCTION

Barometric altimeters along with radar altimeters have been used to aid Inertial Navigation Systems (INS) in order to stabilize the vertical position estimates for applications in aviation [3,4]. For human motion characterization, barometric altimeters have been used in classifying the vertical movement patterns into moving up, down, or remaining level [1,2]. Recently, a pedestrian navigation system integrating GPS, MEMS IMU (Inertial Measurement Unit), barometric altimeter, and transponder demonstrated stable indoor/outdoor pedestrian position tracking, in which a barometric altimeter and transponders were used to stabilize dead-reckoning of IMU indoors [6]. In this paper, we demonstrate drift-free high-resolution vertical positioning using MEMS IMU fused with complementary MEMS barometric altimeter for indoor/outdoor applications under dynamics typical for human movements. Using a low-cost MEMS Attitude and Heading Reference System (AHRS) with integrated GPS and barometric altimeter, we show how a barometric altimeter can be used to stabilize the drift-prone double-integration of accelerometer signals in real-time, while retaining the highly dynamic and responsive characteristic of the accelerometers which is useful in identifying different movements. In this article we focus on tracking relative changes in height, and not the absolute height, in order to isolate the error sources. Absolute height calibration can be performed using GPS or other methods [6]. The barometric altimeter is sensitive to fluctuations in atmospheric pressure which often results in undesired height drift. We use a reference barometric altimeter as a possible solution to mitigate the weather effects.

The performance of height tracking is compared against a reference system consisting of a tactical-grade IMU. This system enables measurement of accuracy on sample-by-sample

basis and helps to optimize the Kalman filter that fuses the individual sensor signals. Since the reference system also measures the orientation error, the effect of orientation error on the height estimation is also analyzed.

II. METHODS

A. System Description Overview

We use an Xsens MTi-G sensor, which is a miniature MEMS Attitude and Heading Reference System (AHRS) containing 3D gyroscopes, 3D accelerometers, 3D magnetometers, a GPS receiver and a barometric altimeter. Since we are mainly interested in demonstrating the fusion of accelerometer and the barometric altimeter, we ignore the GPS data and only consider the orientation, accelerometer, and barometer data. The approach will be to compute the change in height by double-integrating accelerometer signal and stabilizing it with the relative height measurement obtained from a barometric altimeter using a Kalman filter. We show that this combination gives stable high-resolution height measurements under dynamic conditions typical of human movements. Although it is possible to use the absolute altitude information from the GPS receiver to calibrate the relative barometric height measurements, we confine ourselves to tracking relative changes in height.

B. Integration of acceleration

The accelerometer signal (\mathbf{y}_{acc}) contains the acceleration minus the gravity vector in the sensor frame. The vertical acceleration is computed by considering the accelerometer signal in the direction of the vertical and adding the acceleration due to gravity;

$$a = {}^s\mathbf{z} \cdot \mathbf{y}_{acc} + g = |{}^s\mathbf{z}| |\mathbf{y}_{acc}| \cos \theta + g \quad (1)$$

where ${}^s\mathbf{z}$ is the direction of the vertical vector in the sensor reference frame obtained from the AHRS directly. The parameter g is the local value of the acceleration due to gravity, and θ is the angle between \mathbf{y}_{acc} and ${}^s\mathbf{z}$. The acceleration vector in the sensor frame, however, contains bias and gain errors due to temperature calibration errors, bias instability, and etc. The effect of those errors on the net vertical acceleration in the global frame can be visualized in Fig. 1. Note that the situation depicted is at rest, thus no net acceleration is present.

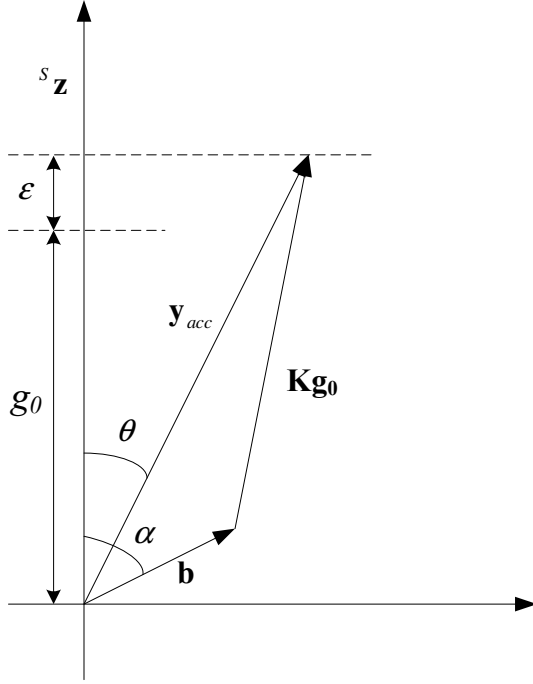


Figure 1: The effect of accelerometer bias and gain error on the net vertical acceleration.

Here the temperature calibrated accelerometer signal is modeled as;

$$\mathbf{y}_{acc} = \mathbf{K}\mathbf{g}_0 + \mathbf{b} + \mathbf{n} \quad (2)$$

where \mathbf{g}_0 is the true gravity vector that would be measured in the sensor frame if there were no calibration errors, \mathbf{K} is the gain error also expressed as $\mathbf{K} = (\mathbf{I} + \mathbf{\Delta})$, with \mathbf{I} the identity matrix and $\mathbf{\Delta}$ a diagonal matrix, \mathbf{b} is the accelerometer bias vector expressed in the sensor frame, and \mathbf{n} is additive white Gaussian noise. The apparent net vertical acceleration, ϵ , including gain and bias errors, is then (ignoring the effect of noise);

$$\begin{aligned} \epsilon &= \mathbf{y}_{acc} \cdot \mathbf{s}_z - g = (\mathbf{K}\mathbf{g}_0 + \mathbf{b}) \cdot \mathbf{s}_z - g \\ &= (\mathbf{I} + \mathbf{\Delta})\mathbf{g}_0 \cdot \mathbf{s}_z + \mathbf{b} \cdot \mathbf{s}_z - (g_0 + \delta g) \\ &= g_0(\cos\theta - 1) + \Delta g_0 \cos\theta + b \cos\alpha - \delta g \end{aligned} \quad (3)$$

where $g = g_0 + \delta g$ is the locally assumed value of acceleration due to gravity. Note that $\Delta = |\mathbf{\Delta}|$ and $g_0 = |\mathbf{g}_0|$. The true magnitude of acceleration due to gravity is g_0 while the error in the assumed value is δg . The first term in (3) is the effect of orientation error, the second term is due to the combination of gain error and orientation error, the third term is the effect of bias, and the last term is the error in assumed value of local acceleration due to gravity. Ignoring the gain error term and using an approximation $\cos\theta \approx 1 - \theta^2/2$ leads to;

$$\epsilon = -\frac{g_0\theta^2}{2} + b \cos\alpha - \delta g \quad (4)$$

For typical human movements, the acceleration due to gravity is the dominant component in the accelerometer signal, causing \mathbf{s}_z and \mathbf{y}_{acc} to be roughly parallel in Fig. 1. Because of this, the small-angle approximation for the cosine function dictates that small errors in inclination have only a moderate effect on the computed vertical acceleration than the horizontal acceleration. In the presence of large horizontal acceleration, however, even a small orientation error would give a sizable error in the vertical acceleration. Heading errors have no adverse effect for height estimation.

The projection of accelerometer bias vector on the vertical, however, is directly proportional to the magnitude of the bias vector. An accelerometer with bias instability of 1 mg can still yield $\frac{1}{2} (0.01\text{m/s}^2)(100\text{s})^2 = 50$ m of large height drift only after 100 seconds. Likewise, the under- or over-estimation in the local value of acceleration due to gravity, δg , also has a direct effect on the net acceleration estimation. We shall see that those components dominate the error in height estimation when the accelerometer noise is not an important factor. In the absence of orientation error, accelerometer gain error, and accelerometer bias, the height error would be purely due to the random walk process of the accelerometer noise. In this case, the standard deviation of the height error is a second-order random walk process whose standard deviation is characterized by $\sigma(t) = \sigma t^{3/2} \sqrt{t/3}$, where σ is the noise density of the accelerometer, t is the time, and T is the sample period.

Thus the accelerometer bias and local value of acceleration due to gravity are important parameters which need to be accurately estimated in order to obtain reasonable performance. In a tightly-coupled system of IMU and barometric altimeter, those parameters can be estimated as a Kalman state, but since we are limiting ourselves here to a loosely-coupled system we treat the accelerometer bias and the local value of acceleration due to gravity as constants which need to be estimated beforehand. The accelerometer bias and acceleration due to gravity can be estimated from measuring several static orientations and assuming the model in (2).

C. Relative Barometric Height Measurement

When the pressure sensor is used as altimeter that measures change in height, the pressure as measured in Pascal is converted to change in height in meters by [5];

$$\Delta h = 44330 \cdot \left(1 - \left(\frac{P}{P_0} \right)^{0.19} \right) - h_{init} \quad (5)$$

where h_{init} is calculated at P_{init} and P_0 is the standard pressure defined as 101.325 kPa. The height measurement contains thermal noise and a significant amount of quantization noise due to a relatively coarse resolution of about 0.2 m. These give the overall noise standard deviation of about 1 m at an update rate of 7 Hz. In order to obtain an accuracy of 0.1 m using the barometric altimeter alone, several seconds of averaging

would be necessary. Therefore, relatively high noise level and low update rate make it unsuitable for tracking highly dynamic movements, but it is still useful for stabilizing the drift-prone accelerometers.

D. Barometric Height Correction using Reference Barometer

During unstable weather the atmospheric pressure fluctuations can easily result in a few meters per hour of drift in terms of height. The altitude obtained from GPS or updates from other sources like transponders can be used to correct for these effects [6], but here we consider the possibility to deploy a reference barometric altimeter which is left stationary to monitor any local fluctuations in altitude due to fluctuations in atmospheric pressure. With a reference barometer, the relative change in height can be accurately tracked reliably for longer periods.

E. Fusing Information using Two-state Kalman Filter

In order to fuse both measurements using a Kalman filter, the above equations have to be related in a state-space format. The two Kalman states are chosen to be the height and the velocity. In state-space, the integration of vertical acceleration to position is expressed as;

$$\begin{bmatrix} h_t \\ v_t \end{bmatrix} = \begin{bmatrix} 1 & T \\ 0 & 1 \end{bmatrix} \begin{bmatrix} h_{t-1} \\ v_{t-1} \end{bmatrix} + \begin{bmatrix} \frac{1}{2} a_t T^2 \\ T a_t \end{bmatrix} \quad (6)$$

where h is the height, v is the vertical speed, T is the sampling period of the accelerometer, and a is the vertical net acceleration in the global frame. The sample period was chosen to be 0.005s (200 Hz). Note that it is important to estimate the bias on the accelerometer signal and compensate for it. The altimeter signal, h_{baro} , is modeled as zero-mean additive white Gaussian noise process with a standard deviation of 1 m.

$$h_{baro} = h_t + w_t, \quad w \sim N(0, 1 \text{ m}) \quad (7)$$

The accelerometer signal is also modeled as zero-mean additive white Gaussian noise with standard deviation of 0.008 m/s².

F. Experimental Procedure

Two experiments were designed to test and analyze the performance of height tracking, with the first experiment focusing on error analysis and the second experiment focusing on application to indoor height tracking of humans.

Experiment 1 (high-resolution error analysis)

An Xsens MTi-G sensor was fixed to a tactical-grade IMU which is used as a reference height measurement (Fig. 2), and the calculated heights were compared. The reference IMU is equipped with a 3-axis fiber-optic gyroscope (FOG) with 3-axis servo accelerometers, which achieves an orientation drift (measured in terms of angle random walk standard deviation) of 0.1 deg./hr. The reference height is calculated by double-

integration of the vertical acceleration given by the reference IMU. Since this method also allows the orientation error of the MTi-G to be tracked, the influence of orientation error on the height estimation can be analyzed. A second barometric altimeter is left stationary to be used as reference barometer.

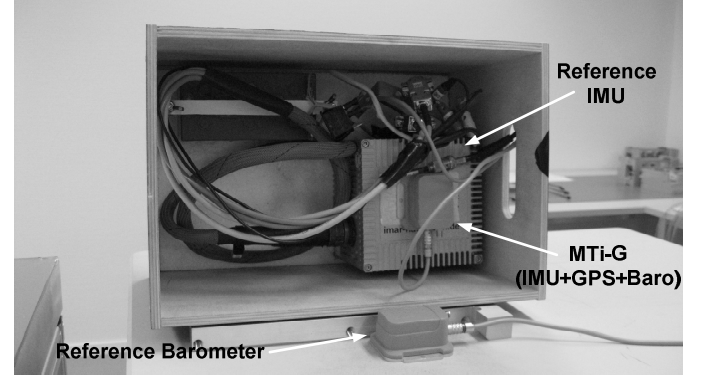


Figure 2: Xsens MTi-G AHRS sensor mounted on tactical-grade IMU for high-resolution height error analysis. Second MTi-G sensor is used as a reference barometric altimeter.

Experiment 2 (stability analysis under human movements)

To test the height stability and accuracy under typical human motion (walking) in an indoor office environment, an Xsens MTi-G was strapped to the chest (Fig. 3) and walked up and down a staircase with a landing halfway up the stairs. The height difference was known (3.42 m). A second sensor, again, is used to monitor any drift in height as result of atmospheric pressure variation during the experiment.



Figure 3: Xsens MTi-G AHRS Sensor strapped to the chest for height tracking during walking up and down a staircase.

III. EXPERIMENTAL RESULTS

A. Experiment 1 (high-resolution error analysis)

The IMU signals (accelerometer and gyroscope magnitudes) during the experiment are shown in Fig. 4, clearly distinguishing the periods of motion and no motion. After 20 seconds of rest at the table height (1.10 m above the floor), the sensor was lifted off the table and moved up and down rapidly for about 8 seconds with vertical displacement of

approximately ± 0.50 m and returned to the original position and orientation for 10 seconds. The sensor was then lifted from the table again and brought down nearly to the floor and hoisted up to about 2 meters and then brought back to the original position and orientation.

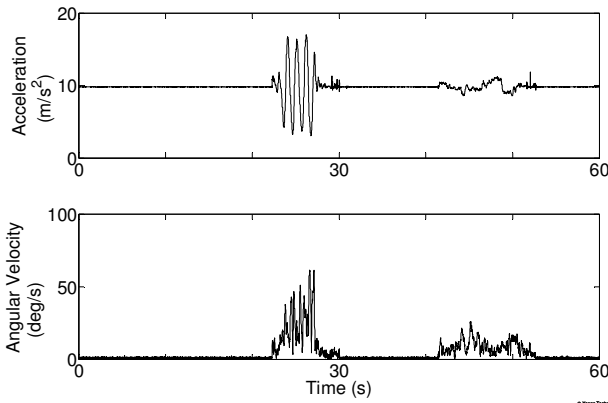


Figure 4: Acceleration and angular velocity magnitude signal during Experiment 1.

The sensor orientation during the movement, in terms of Euler angles (roll, pitch, and yaw), is shown in Fig. 5. The maximum inclination experienced during the experiment was about 10 degrees.

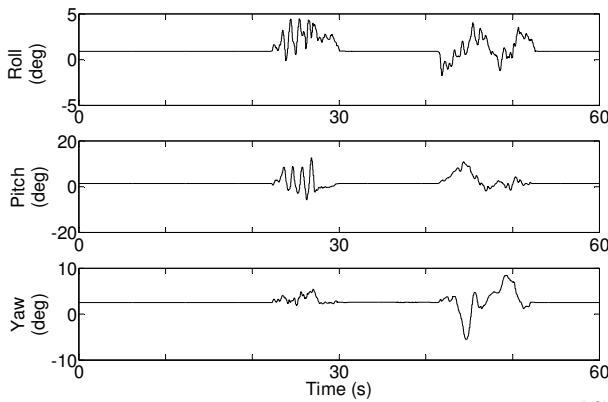


Figure 5: Euler angles (orientation) of the sensor during Experiment 1. Shown are roll (above), pitch (middle), and yaw (below).

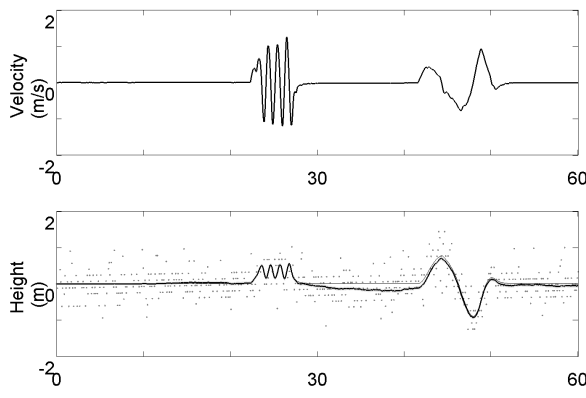


Figure 6: Velocity (above) and height (below) comparison. For the height plot, the reference height from a tactical-grade IMU (thin line) and MTi-G

G (thick line) are compared. The height obtained from the MTi-G is stabilized by the barometric-altimeter and the barometer drift due to change in atmospheric pressure is compensated using the reference barometer. The barometric altimeter samples are shown in dots.

The vertical velocity and position results are shown in Fig. 6. In the height plot (below) the heights obtained using the reference IMU and the MTi-G are compared. The height error remained within about ± 0.2 m throughout the experiment (also see Fig. 7). Note that the barometric altimeter signal used to stabilize the height for the MTi-G has been corrected for height drift due to change in atmospheric pressure. Furthermore, for both the reference IMU and MTi-G, the accelerometer bias has been estimated from a bias estimation procedure performed just before the experiment. This procedure estimates the accelerometer bias from multiple static orientation measurements. The estimated bias was subtracted from the accelerometer signal for height estimation.

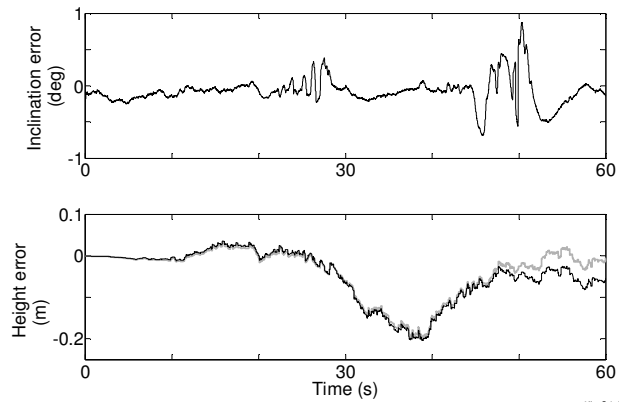


Figure 7: Inclination error (above) and height error (below). For each plot, the reference inclination/height is obtained from a tactical-grade IMU. The gray line in the height error plot (below) shows the height error when the inclination error is eliminated.

Figure 7 shows the inclination error and height error during the movement. The reference orientation and height were obtained from the reference IMU whose orientation has been compensated for the rotation rate of the Earth. The inclination error during the experiment remained less than one degree, which is about the expected accuracy of MEMS-based low-cost AHRS under the given conditions.

The corresponding height error plot in Fig. 7 suggests very little correlation between the inclination error and height error. In fact, when the orientation error is eliminated from the MTi-G (by using the orientation from reference IMU), the difference in height output shows very little change (shown by the gray line Fig. 7). This follows from the theoretical expression (4) in which the error in the vertical acceleration is quadratic in inclination error (inclination error is usually much smaller than unity). This result implies that the error in height is almost entirely due to the residual accelerometer bias for this experiment.

In this experiment, we have tried to isolate the error contribution from barometer drift by making use of a reference

barometric altimeter which remained stationary during the experiment. Figure 8 shows the height calculated with and without the reference barometer. The benefits of using a reference barometer can clearly be seen in this figure. The measured rate of pressure change during the experiment was approximately +190 Pascal/hr (or -16 m/hr in height), which corresponds to the transition between stable good weather and unstable high pressure system [5].

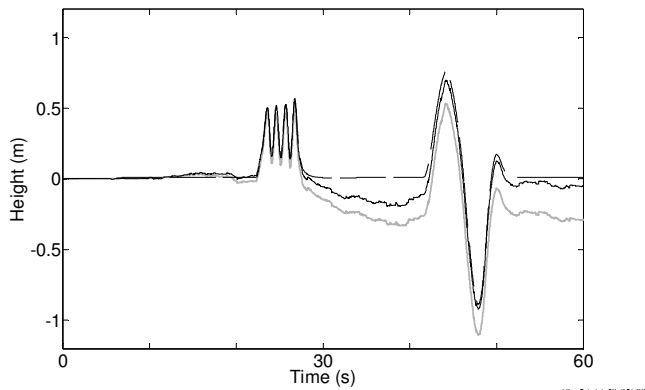


Figure 8: Height with barometer drift compensation using a reference barometer (solid) and without correction (grey). The reference height from a tactical-grade IMU is also shown by the dashed line.

B. Experiment 2: Stability under walking motion

In this experiment, the MTi-G sensor was strapped to the chest as shown in Fig. 3 and a staircase with a landing was walked up and down. Figure 9 shows the accelerometer and gyroscope magnitudes during the experiment. The starting position is marked by the first 7 seconds of no motion. The second floor was reached around 30 seconds after and five squats were performed between 35 and 42 seconds. The rest of the measurement was walking down the same flight of stairs and coming to rest at the initial position.

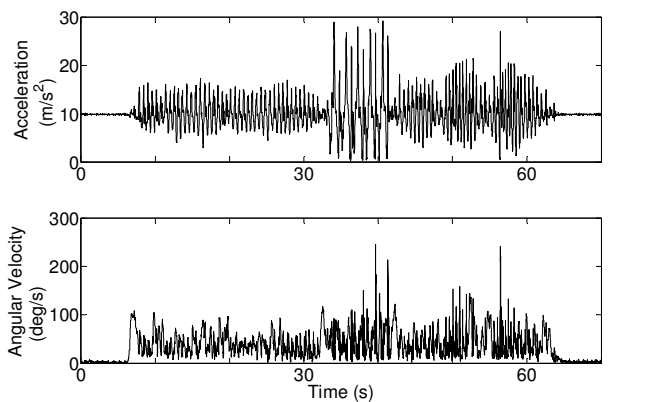


Figure 9: Accelerometer and gyroscope magnitude data captured during walking up and down a staircase.

The corresponding vertical velocity and height after fusion of accelerometer and barometric altimeter are shown Fig. 10, in which the actual height difference of 3.42 m has been marked by the dotted lines. Note that the footsteps are clearly visible in

the velocity plot. Steps taken while actually walking up and down the stairs can be distinguished from steps taken while remaining level in the velocity plot. Note also that the calculated height has been compensated for the measured pressure drift rate of -93 Pa/hr (characterized by stable rainy weather [5]). This rate corresponds to +7.7 m/hr. Accelerometer bias measurements were performed before and after the experiment, in which six static orientations were measured.

A good stability of height estimation can be seen by comparing the height just before and after the squat. At those times, the height difference with respect to the initial height is nearly equal the actual height difference between the first and second floor.

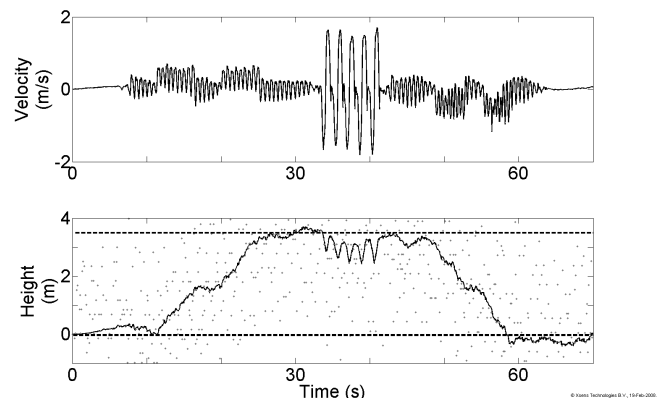


Figure 10: Height estimation stabilized by barometric altimeter when walking up and down a flight of stairs (with squatting five times on the second floor). Reference barometer is used to correct for barometric drift.

IV. CONCLUSION

We have demonstrated drift-free high-resolution vertical positioning by fusing MEMS accelerometers with complementary MEMS barometric altimeter. This low-cost, low-power, and small form factor system enables high-resolution vertical positioning in real-time under dynamics typical of human movements. In the first experiment, a tactical-grade IMU was used to measure height errors and showed that the height error was bounded by +/- 0.2 m after correcting for the drift in barometric altimeter reading due to fluctuations in atmospheric pressure. It was also confirmed that the orientation error has a rather minor effect on the height accuracy as long as the orientation error is not too large and that the movements do not contain significant horizontal acceleration. Under those conditions the accelerometer bias was identified to be the most critical factor in obtaining good vertical accuracy. The second experiment, in which the integrated sensor was strapped to the chest, showed good accuracy and stability while walking up and down a staircase. This system can be easily augmented by GPS or other means such as transponders to enable absolute height measurement. It was demonstrated that the use of reference barometric

altimeter, if available, can be a viable option in eliminating the height drift due to change in the atmospheric pressure.

V. DISCUSSION

In this paper, we deliberately decoupled the orientation estimation and height estimation for facilitating the error analysis, but they could be integrated into a tightly-coupled system in which the accelerometer bias can be estimated as an additional Kalman state. Since the bias of MEMS accelerometers do change with time due to inherent bias instability, temperature, and other effects, it would be highly desirable to estimate it as a Kalman state.

In the error analysis, the inclination error played a minor role in contributing to the height error compared to the gain and bias errors. The amount of inclination error, however, highly depends on the type of movement the sensors experience, and it may lead to significant orientation error during certain kind of movements. In that case, the orientation error would, of course, be an important factor in the height error.

VI. ACKNOWLEDGEMENTS

This publication has been supported by EC-contract FP6-IST-34120, Action line 2.5.2 Micro based subsystems. The support is greatly acknowledged. This publication reflects only the authors' views. The European Community is not liable for any use that may be made of the information contained therein.

REFERENCES

- [1] Sagawa, K.; Ishihara, T.; Ina, A.; Inooka, H, *Classification of human moving patterns using air pressure and acceleration.*, Industrial Electronics Society, 1998. IECON '98. Proceedings of the 24th Annual Conference of the IEEE Volume 2, 31 Aug.-4 Sept. 1998 Page(s):1214 - 1219 vol.2
- [2] Sagawa, K.; Inooka, H.; Satoh, Y, *Non-restricted measurement of walking distance.*; Systems, Man, and Cybernetics, 2000 IEEE International Conference on, Volume 3, 8-11 Oct. 2000 Page(s):1847 - 1852 vol.3
- [3] Gray, R.A.; Maybeck, P.S., *An integrated GPS/INS/baro and radar altimeter system for aircraft precision approach landings*; Aerospace and Electronics Conference, 1995. NAECON 1995., Proceedings of the IEEE 1995 National Volume 1, 22-26 May 1995 Page(s):161 - 168 vol.1
- [4] R. G. Brown and P. Y. C. Hwang, *Introduction to Random Signals and Applied Kalman Filtering*, 3rd Edition, Wiley & Sons, 1997, ISBN 0-471-12839-2
- [5] VTI Technologies Application Note: SCP1000-D01(E)/D11(E) Pressure Sensor
- [6] Weimann, F, Abwerzger, G, and Hofmann-Wellenhof, B. *A Pedestrian Navigation System for Urban and Indoor Environments*, Proceedings ION GNSS 2007.